



Sediment loading from the Río de la Plata as a driver of regional sea-level variability

Alessio Rovere ^{a,b,*}, Tamara Pico ^c, Gabriel Tagliaro ^d, Ciro Cerrone ^{a,e}, Luca Lämmle ^f, Archimedes Perez Filho ^f, Karla Rubio-Sandoval ^g, Luigi Jovane ^d, Jerry X. Mitrovica ^h, Christopher G. Piecuch ⁱ, Giovanni Scicchitano ^j

^a Department of Environmental Sciences, Informatics and Statistics, University of Venice Ca' Foscari, Mestre, Italy

^b Center for Marine Environmental Sciences, MARUM, University of Bremen, Germany

^c Department of Earth and Planetary Sciences, UC Santa Cruz, Santa Cruz, 95064, CA, United States

^d Instituto Oceanográfico, Universidade de São Paulo, Praça Do Oceanográfico, 191 05508-120, São Paulo, SP, Brazil

^e International Centre for Climate Change Research and Studies (CSRCC), Franchetti Palace, San Marco 2847, 30124, Venice, Italy

^f Department of Geography, Institute of Geosciences, University of Campinas (UNICAMP), 13083-855, Campinas, Brazil

^g Instituto de Geociencias, Universidad Nacional Autónoma de México, Querétaro, Mexico

^h Department of Earth and Planetary Sciences, Harvard University, 20 Oxford Street, 02138, Cambridge, Massachusetts, USA

ⁱ Woods Hole Oceanographic Institution, Woods Hole, Massachusetts, USA

^j Department of Earth and Geo-Environmental Sciences, University of Bari Aldo Moro, Via Orabona, 4, 70125, Bari, Italy

ARTICLE INFO

Editor: J.P. Avouac

Keywords:

Sea level
Sediment isostasy
Last interglacial
Río de la Plata

ABSTRACT

Sea-level reconstructions are critical benchmarks for testing models of ice-sheet stability and climate change. Their interpretation, however, is complicated by sea-level changes driven by different processes, among which include the solid Earth's response to sediment loading. Here we show that incorporating sediment isostatic adjustment reduces long-standing discrepancies among Marine Isotopic Stage (MIS) 5a and 5e records from the Río de la Plata estuary by up to an order of magnitude, indicating that regional sedimentary histories can shift relative sea-level estimates by several meters compared to traditional glacial isostatic adjustment-based approaches. We further emphasize how sediment loading may play an important role in influencing relative sea level throughout the Holocene and may continue to affect regional modern tide-gauge records. These findings underscore the importance of regionally resolved sedimentation histories, in contrast to approaches based solely on global compilations, and highlight the need for expanded shelf coring and seismic surveys.

1. Introduction

Reconstructing global mean sea-level (GMSL) changes over Quaternary timescales requires disentangling the processes that drive sea-level change (Rovere et al., 2016; Gregory et al., 2019). To estimate GMSL during past periods of the Earth's history, relative sea-level (RSL) records derived from direct sea-level proxies must first be corrected for local processes that drive vertical displacement, such as tectonics, mantle dynamic topography (vertical deflections of Earth's surface and sea surface caused by the slow, time-dependent flow within the mantle, Braun (2010), Austermann et al. (2017), Stephenson et al. (2019), Rovere et al. (2023), and glacial isostatic adjustment due to ice and ocean loading.

Isostatic adjustments caused by the redistribution of surface mass loads on Earth can produce significant deviations in relative sea level across a wide range of timescales. Glacial Isostatic Adjustment (GIA)

refers to the response of the Earth to variations in ice and ocean mass loading (Farrell and Clark, 1976). The magnitude of this response depends both on the history of ice and ocean loading and on the rheological structure of the mantle (Milne and Mitrovica, 1998). GIA can generate substantial departures from GMSL, even at far-field sites located well away from former ice margins (Lambeck and Chappell, 2001). Although GIA is by far the most studied isostatic process in sea-level science, research has also examined the role of other forms of isostatic adjustment and associated sea level change, including those caused by karst dissolution (Adams et al., 2010; Creveling et al., 2019), reef growth (Rovere et al., 2023; Lin et al., 2023), and sediment redistribution along continental shelves (Pico, 2020; Ferrier et al., 2015; Dalca et al., 2013; Pico et al., 2016).

The sea-level response to sediment loading and compaction has long been recognized as a potentially important signal in regional sea level

* Corresponding author.

E-mail address: alessio.rovere@unive.it (A. Rovere).

<https://doi.org/10.1016/j.epsl.2026.119996>

Received 19 December 2025; Received in revised form 10 March 2026; Accepted 18 March 2026

Available online 4 April 2026

0012-821X/© 2026 The Authors. Published by Elsevier B.V. This is an open access article under the CC BY license (<http://creativecommons.org/licenses/by/4.0/>).

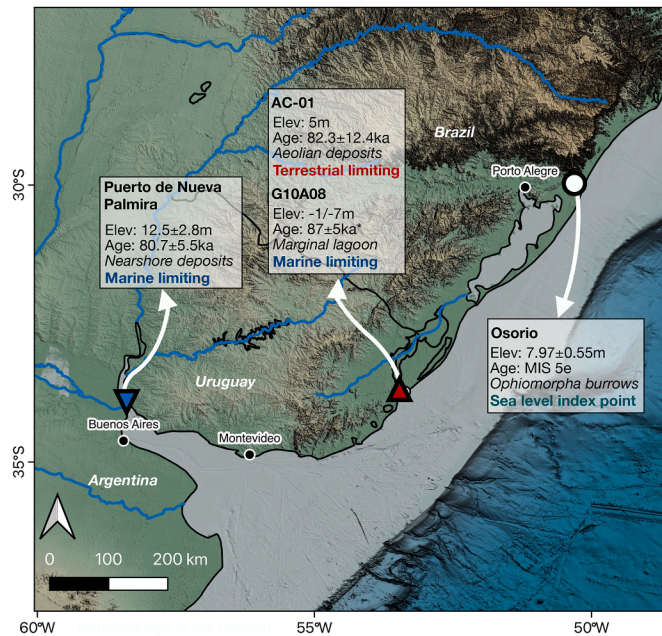


Fig. 1. Coastal area and continental shelf between Uruguay and Brazil (Rio Grande do Sul State), with data on MIS5a and MIS5e sites as reported by Tomazelli and Dillenburg (2007), Rojas and Martínez (2016), Lopes et al. (2024). Blue and red triangles represent, respectively, marine and terrestrial limiting data points. Background map data from GMRT (Ryan et al., 2009).

records through time (e.g., Reynolds et al., 1991; Simms et al., 2013). Subsidence (sinking of land that results in sea-level rise) from sediment compaction, particularly in large deltaic systems (e.g., the Mississippi Delta; Törnqvist et al., 2008) may reach several millimeters per year. However, sediment loading has only recently been incorporated into a gravitationally self-consistent global sea-level model (Dalca et al., 2013; Ferrier et al., 2017; Pico et al., 2016). Incorporating the sea level response to sediment erosion and deposition in major river deltas with high sediment fluxes, such as the Indus River delta (Ferrier et al., 2015) and Yellow River delta (Pico et al., 2016), has been shown to be important for accurate estimates of GMSL since the Last Interglacial (125 ka). Pico (2020) used global sediment fluxes to simulate delta deposition globally to assess the sea level response to sediment loading since 122 ka and found that at some sites sediment loading caused relative sea level excursions of ~15 m, although there was no statistically significant global signal of sediment loading in the observed elevation compilation of Last Interglacial (MIS 5e; 129–116 ka) sea-level proxies.

In this work, we focus on the isostatic adjustment and associated sea level signal generated by sediment loading on the continental shelf of the Río de la Plata (Argentina and Uruguay). We use sedimentary core and bathymetric data to build a sediment loading scenario and calculate the sea-level response since 122 ka in the region. We show that incorporating sediment isostatic adjustment (SIA) alongside glacial isostatic adjustment (GIA) reduces apparent discrepancies among sea-level index points (SLIPs) dated to Marine Isotopic Stage (MIS) 5a (80 ka) and improves the fit between MIS 5e (125 ka) observations and prior GMSL estimates. We emphasize in our results that the SIA may also influence regional Holocene and modern sea-level observations.

2. Geological and sea-level context of the Río de la Plata

The Río de la Plata region is located on a passive margin (overview of the regional geodynamics in Pedoja et al. (2011b) and references therein) and is shaped by vast sediment inputs, offering a unique setting to evaluate the impact of sediment isostatic adjustment on relative sea-level reconstructions. The Río de la Plata estuary, formed by the

Uruguay and Paraná rivers, drains the fifth-largest basin globally (more than 3 million km²; Laborde and Nagy, 1999) and is associated with one of the world's largest submarine fan-like features (Tagliaro et al., 2024). Together, the Uruguay and Paraná rivers deliver an annual mean flow of 22,000 m³ s⁻¹ and transport between 120 and 199 million tons yr⁻¹ of fine sands, silts, and clays (Depetris and Griffin, 1968; Amsler and Drago, 2009; Fossati et al., 2014), which are dispersed across the SW Atlantic via the Malvinas current and deposited on the continental shelf offshore Argentina, Uruguay and southern Brazil (Perez et al., 2016; Michaelovitch De Mahiques et al., 2021).

The coastal plains built by these sediments preserve a rich record of past sea-level positions. Along the southern coasts of Brazil, deposits extend back at least to Marine Isotope Stage (MIS) 7 (~240 ka) (Lopes et al., 2014; Guedes et al., 2020). MIS 5e (~125 ka) deposits are typically associated with the Pleistocene beach barrier known as "Barreira III" (Tomazelli et al., 2006; Tomazelli and Dillenburg, 2007; Villwock, 1984), which lies 7–10 m above present sea level (see the Supplementary Materials for details). Recent work (Lopes et al., 2024) suggests that Barreira III (that outcrops at Osório at ~8 m above sea level, Fig. 1) was reoccupied during MIS 5a and MIS 5c (~82 and ~96 ka, respectively; Fig. 1).

Analysis of relative sea-level (RSL) data reveals an apparent discrepancy. Pedoja et al. (2011b,a) noted that outliers in Pleistocene uplift rates between Brazil and Patagonia may be due to sediment loading and its associated isostatic response. At the mouth of the Río de la Plata, MIS 5a RSL reached at least 12.5 m above present (as indicated by a nearshore fossil-rich deposit at Puerto de Nueva Palmira; Martínez et al., 2001), whereas ~450 km to the east, in the Chuy Creek area (sites AC-01 and G10A08; Lopes et al., 2020, 2024), marine deposits and aeolian sediments range from -7 to +5 m, likely reflecting reoccupation or reworking of MIS 5e deposits (e.g., Osório; Fig. 1, see the Supplementary Materials for details). The discrepancy between these constraints (i.e., the marine limiting indicator should not be at higher elevation than the terrestrial limiting indicator) indicates differential post-depositional vertical displacement at these two sites. Here we test the hypothesis that this apparent discrepancy can be resolved by considering sediment isostatic adjustment processes.

3. Methods

To evaluate the role of isostatic processes in the Río de la Plata region, we correct direct sea-level proxies with predictions from ensembles of GIA and SIA models. The GIA simulations sample a variety of parameters for lithospheric thickness, upper- and lower-mantle viscosities, and ice-sheet configurations, following approaches previously applied to MIS 5e reconstructions (Dyer et al., 2021). GIA contributions are reported as the mean $\pm 1\sigma$ across the 576 model outputs of Dyer et al. (2021). For SIA, we developed a model of sediment loading since 122 ka by integrating bathymetry data with published core-derived sedimentation rates based on Late Pleistocene sediment ages (Supplementary Table 1, Supplementary Figure 1). We performed simulations to calculate the impact of sediment loading on relative sea level as in Ferrier et al. (2015), Pico et al. (2016).

3.1. Glacial isostatic adjustment

Relative sea-level changes are influenced by glacial isostatic adjustment (GIA), that is, the response of the Earth to changes in ice and ocean mass loading (Farrell and Clark, 1976). The magnitude of this response depends on both the history of ice and ocean loading and the rheological properties of the mantle (Milne and Mitrovica, 1998). GIA can cause substantial deviations from global mean sea level (GMSL), even at far-field sites located away from former ice margins (Lambeck and Chappell, 2001).

To quantify the GIA contribution to RSL at our study sites, we use 576 GIA predictions from the models developed by Dyer et al. (2021).

These models explore variations in the Earth's viscosity structure and ice sheet configurations, and are based on the density and elastic structure from [Dziewonski and Anderson \(1981\)](#). Specifically, the models vary uniform values for the upper mantle viscosity, lower mantle viscosity, and effective elastic lithospheric thickness. The upper mantle extends from the base of the lithosphere to 660 km depth, while the lower mantle lies between this boundary and the core-mantle interface. The model ensemble includes lithospheric thicknesses of either 71 or 96 km, upper mantle viscosity from 0.3 to 0.5×10^{21} Pa-s, and lower mantle viscosity from 3 to 40×10^{21} Pa-s.

The ice models employed by [Dyer et al. \(2021\)](#) use the ICE-6G reconstruction for the last deglaciation ([Peltier et al., 2015](#)), and follow the global sea-level curve of [Waelbroeck et al. \(2002\)](#) prior to the Last Glacial Maximum (LGM), shifted back by 3.5 ka to align with coral-based constraints (see [Dyer et al., 2021](#)). To account for uncertainty in deglacial timing, two eustatic sea-level curves were tested: one with the MIS 6 glacial maximum (minimum sea level) at 135.5 ka, and one at 142 ka. It is worth noting that these parameters have limited influence beyond MIS 5e. The GIA simulations were run with three distinct ice sheet configurations: (1) a reconstruction assuming MIS 6 ice extent equivalent to MIS 2, with a Laurentide Ice Sheet (LIS) volume of 89 m sea-level equivalent (SLE); (2) a reconstruction with a larger Fennoscandian ice sheet and an LIS volume of 59 m SLE ([Lambeck et al., 2006](#)); and (3) a configuration with an even larger Fennoscandian ice sheet and an LIS volume of 43 m SLE ([Colleoni et al., 2016](#)).

3.2. Sediment isostatic adjustment

To account for the effects of sediment loading, we estimated sediment thickness using core data and modern bathymetry. We first compiled published core records ([Lantzsch et al., 2014](#); [Pereira De Ávila et al., 2020](#), Supplementary Table 1) and then extrapolated the sedimentation rates to model a cumulative sediment thickness since the LIG. We represented regional topography by generating a 10-cell width smoothed map from modern bathymetry ([Alberoni et al., 2020](#)). Lastly, we scaled the smoothed surface to match the cumulative sediment thickness at the core locations. The resulting sediment thickness model represents the best possible estimate given current data constraints (Supplementary Figure 1).

The sediment thickness model is based on two main assumptions: (1) that the general sediment distribution patterns across the Uruguayan and southern Brazilian shelves since the Pleistocene resemble modern patterns as expressed in bathymetry data; (2) that sedimentation rates at core locations are continuous since MIS5e (122 ka). These assumptions allow us to consider modern bathymetry as an analogue to MIS5e paleo bathymetry, and to extrapolate published Late Pleistocene sedimentation rates into the MIS5e.

To construct a sediment loading history since MIS 5e (122 ka), we apply a sediment loading rate from 122 ka to 10.5 ka, which represents our glacial sedimentation scenario ([Fig. 2A](#)). After the Holocene (10.5 ka), we apply a different sediment loading rate, which includes sedimentation in the estuary, as would have occurred during times of higher sea level ([Fig. 2B](#)). To conserve mass, we identify the aerial extent of the Paraná River drainage basin and uniformly remove a layer of sediment with a volume equivalent to the sediment flux deposited in the oceans. This procedure accounts for the density difference between marine sediments (1750 kg m^{-3}) and terrestrial sediments (2650 kg m^{-3} , [Bahr et al., 2001](#)). Given the uncertainty on sedimentation rates over the last glacial cycle, we consider our reconstructed sediment thickness model derived from core data and modern bathymetry as an upper bound (100% scenario). We also considered sediment loading scenarios that decreased the uniform sediment loading rate by a factor of 75%, 50%, and 25%. The resulting sediment deposition over the last glacial cycle for the 100% scenario is shown in [Fig. 5A](#).

To calculate relative sea-level (RSL) change due to sediment isostatic adjustment, we used a gravitationally self-consistent sea-level model.

Our calculations are based on the theory and pseudo-spectral algorithm described by [Dalca et al. \(2013\)](#) with a spherical harmonic truncation at degree and order 512 (spatial resolution of ~ 34 km). Our predictions require models for Earth's viscoelastic structure. We adopted an earth model characterized by a lithospheric thickness of 71 km, and upper and lower mantle viscosities of 3×10^{20} Pa-s and 3×10^{21} Pa-s, respectively. These Earth structure parameters are consistent with Holocene sea level data in Brazil (Supplementary Figure 12), and fall within the range of parameters explored in the ensemble of 576 simulations we use to quantify GIA uncertainty. Our simulations ignore ice and ocean load changes in order to isolate the effect of sediment loading. We note that we ignore sediment compaction, and its effects on porewater volume, as we wish to focus on the relative sea level change due to sediment isostatic adjustment on nearby relative sea level markers (rather than the precise elevation of any location where sediment deposition rates are high).

4. Results and discussion

4.1. Marine isotopic stage 5e

We first assess how the combination of GIA and SIA affects MIS 5e deposits at Osório, where coastal deposits with *Ophiomorpha* ichnofacies mark paleo-RSL at 7.97 ± 0.55 m ([Fig. 3A](#)). Because this facies is highly susceptible to reworking, we assume deposition occurred at the maximum RSL highstand, predicted at ~ 128 ka based on our suite of GIA simulations (Supplementary Figure 2). At this time, GIA contributed 5.7 ± 3.3 m to RSL (Supplementary Figure 3), which must be subtracted from the observed value. A GIA-only correction yields a GMSL range of -1.1 to 5.6 m, whereas adding subsidence from SIA (5.4 ± 2.2 m; mean and standard deviation of 25% to 100% scenarios; Supplementary Figure 4) shifts the estimate to 3.4 - 11.8 m (1σ ; [Fig. 3B](#)). These values align more closely with global reconstructions of MIS 5e sea level, which consistently place GMSL above pre-industrial levels ([Dutton et al., 2015](#)). Recent estimates include a 5-90% confidence interval of 1.2 - 5.3 m ([Dyer et al., 2021](#)), a 68% confidence interval of 3.6 - 8.7 m ([Barnett et al., 2023](#)), and a likely range of 5 - 10 m reported in IPCC AR6 ([Gulev et al., 2021](#)). Within this context, including SIA brings our average MIS 5e GMSL estimate to 7.6 m, which is within the uncertainty range all the previous GMSL estimates.

4.2. Marine isotopic stage 5a

In the study area, the elevation of marine limiting data at Nueva Palmira is higher than the terrestrial limiting at Chuy Creek, contrary to the expectation that marine indicators should lie below terrestrial indicators. What could have caused this discrepancy?

Tectonic motion may provide one possible explanation for the observed mismatch between these MIS 5a limiting points. While the Río de la Plata estuary lies on a passive margin with no evidence of significant Late Quaternary deformation, [Brunetto et al. \(2019\)](#) reported long-term uplift of 0.025 - 0.05 mm yr^{-1} in the central Río de la Plata Craton near Nueva Palmira. These rates, however, are too small to reconcile the observations: the marine limiting indicator at Nueva Palmira requires sea level above $+12.5$ m, while the combination of marine and terrestrial limiting indicators at Chuy Creek (AC-01) requires it to be between -7 and $+5$ m. Tectonics can only explain up to 2 - 4 m of this discrepancy ([Fig. 4](#)).

GIA models for MIS 5a (80 ka) capture part of this regional variability, predicting an average difference of 3.4 m RSL between the two sites (Supplementary Figure 5). In both locations, RSL peaks at 81.5 ka (Supplementary Figure 6), with a GIA correction (departure from GMSL, Supplementary Figure 5) reaching 4.5 ± 2.3 m (total predicted RSL at 80 ka = -18.7 m) at Nueva Palmira and only 1.1 ± 2.1 m at Chuy Creek (Supplementary Figure 5). Yet even this GIA correction does not fully

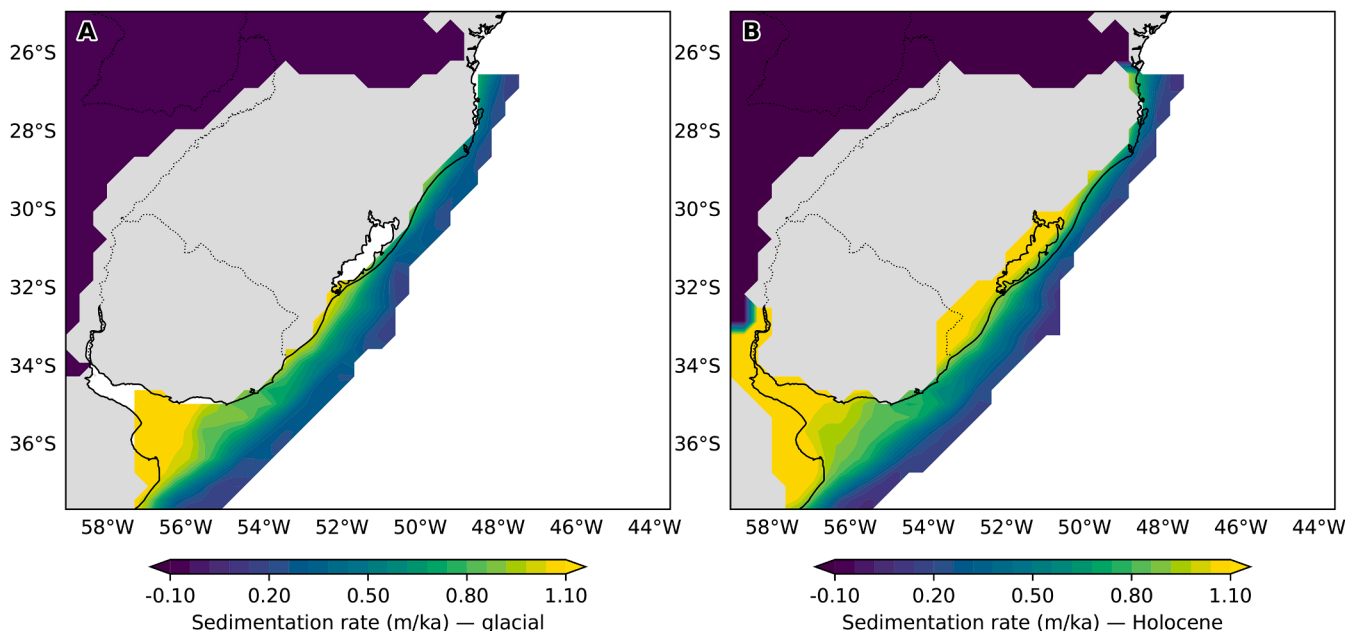


Fig. 2. A. Sedimentation rate applied between 122 ka to 10.5 ka. B. Sedimentation rate applied from 10.5 ka to modern.

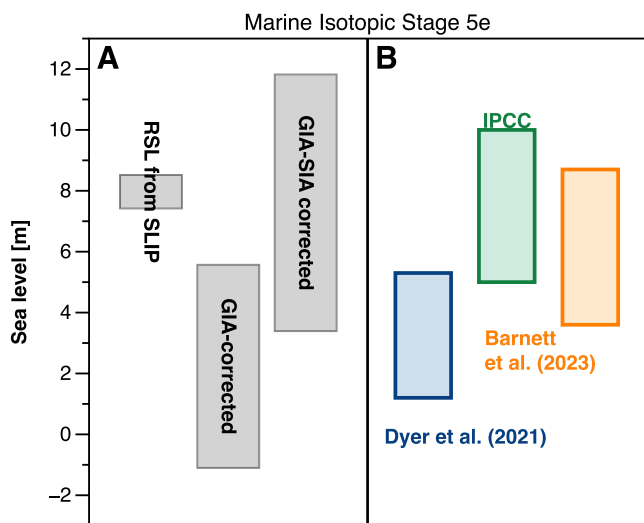


Fig. 3. A. MIS 5e relative sea level (RSL) in Osorio as indicated by (from left to right) uncorrected sea level index point (SLIP), GIA-corrected and GIA + SIA corrected SLIP. B. GMSL in MIS 5e as estimated by Dyer et al. (2021), Barnett et al. (2023) and the IPCC AR6 (Gulev et al., 2021).

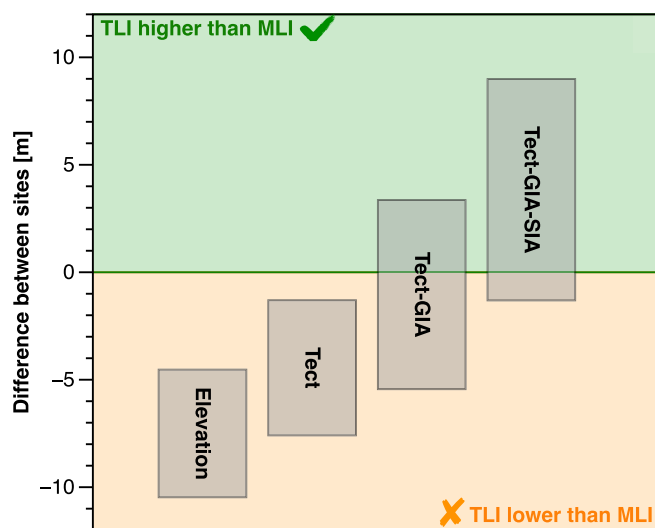


Fig. 4. Difference between the marine limiting index point (MLI) in Nueva Palmira and the terrestrial limiting point (TLI) in Chuy Creek (AC-01) after applying different corrections. From left to right: elevation only, Tectonics only, GIA + Tectonics, GIA + SIA + Tectonics.

reconcile the inconsistency between the MLI at Nueva Palmira and the TLI at Chuy Creek (Fig. 4).

Including SIA resolves the observed disagreement between these two indicators because sediment thickness in our sediment loading scenario (Fig. 5A) is concentrated near the Río de la Plata estuary, and therefore relative sea level due to SIA is greater near Nueva Palmira compared to Chuy Creek (Fig. 5B, Supplementary Figure 7). SIA produces only minor subsidence at Nueva Palmira (2 ± 0.9 m) but substantially greater subsidence at Chuy Creek (5.5 ± 2.7 m), restoring the expected relationship in which the TLI lies above the MLIs (Fig. 4).

Having resolved the relative discrepancy between the MLI at Nueva Palmira and the TLI at Chuy Creek, we next consider what these corrected indicators imply for absolute MIS 5a GMSL. Assuming that GIA, tectonics, and SIA are the dominant drivers of relative sea-level change in this region, our corrections yield a GMSL between -3.9 and +13.4 m

(Supplementary Figure 8). Other processes, such as mantle dynamic topography, may also contribute, but are expected to be less relevant at these timescales (Austermann et al., 2017). The upper bound of this range appears implausibly high, as a GMSL above +10 m would require climate conditions inconsistent with the lower insolation and cooler temperatures of MIS 5a compared to MIS 5e (Supplementary Figure 9). The lower bound, by contrast, is more consistent with the higher end of recent MIS 5a GMSL estimates.

Prior reconstructions based on isotopic records suggest that MIS 5a sea levels were much lower than present-day. Planktonic $\delta^{18}\text{O}$ records from the Red Sea indicate sea levels well below present (~ -20 m), though these may be biased by uncertainties related to converting $\delta^{18}\text{O}$ to global ice volume, including temperature, or even RSL corrections (Grant et al., 2014; Peak et al., 2022). Benthic $\delta^{18}\text{O}$ records also place MIS 5a GMSL tens of meters below present (Spratt and Lisiecki, 2016),

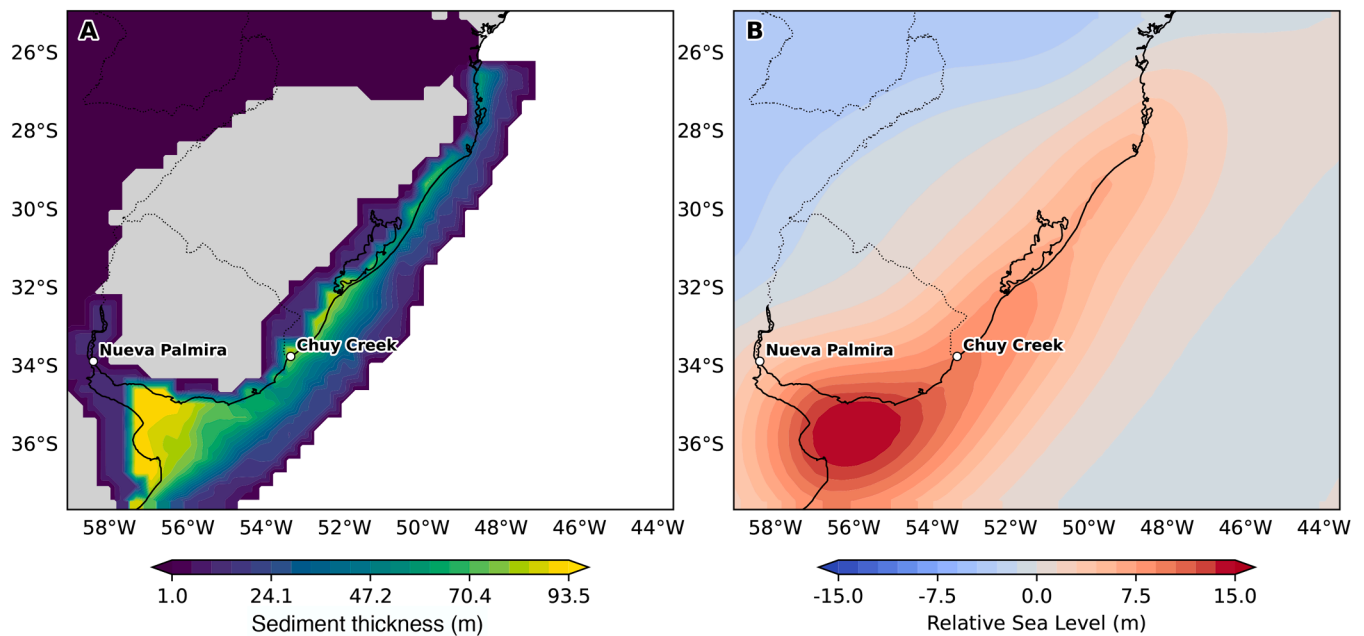


Fig. 5. A. Sediment loading (100% loading scenario) on the Río de la Plata continental shelf between MIS 5a and present-day (100% loading scenario). B. Relative sea-level change (for the 100% loading scenario) since 80 ka caused by sediment isostatic adjustment (SIA). Positive values represent subsidence, negative represent uplift caused by SIA (see standard deviation in Supplementary Figure 7).

but recent work suggests that such reconstructions may be biased by several tens of meters when compared with direct proxies during interstadials (De Gelder et al., 2022; Dalton et al., 2022; Farmer et al., 2023; Pico, 2022).

Indeed, converting $\delta^{18}\text{O}$ to global ice volume requires accurate corrections for ocean temperature (Shackleton et al., 2023), which appear to drop early in the last glacial cycle before substantial ice sheet growth (Shakun et al., 2015; Shackleton et al., 2021), in addition to assumptions about the size and distribution of continental ice sheets (Mix, 1987) and/or the influence of diagenesis (Poirier et al., 2021).

Direct proxy compilations provide a different picture. Though there are relatively few sites compared to MIS 5e, a global review of MIS 5a and 5c proxies found that most index points were above present-day sea level (Thompson and Creveling, 2021). After accounting for tectonic effects, Creveling et al. (2017) inferred MIS 5a GMSL below present (-8.5 ± 4.6 m, or -10.5 ± 5.5 m for well-dated sites), consistent with estimates from the Pacific coasts of North America (Simms et al., 2016; Muhs et al., 2012). More recently, three-dimensional GIA modeling (Thompson et al., 2023) was shown to simultaneously reconcile RSL records across the Atlantic and Pacific coasts of North America and in the Caribbean with a peak MIS5a GMSL value consistent with (Creveling et al., 2017) (-13 m). These bounds overlap with the MIS 5a GMSL range recently inferred from Barbados (-32.5 m to -10.7 m) (Tawil-Morsink et al., 2022).

Towards the lower side of that range, reconstructions from the Huon Peninsula (Papua New Guinea) place peak MIS 5a GMSL at -20 m (De Gelder et al., 2022) (Supplementary Figure 9). Murray-Wallace et al. (2021) estimated GMSL oscillations around -24 to -26 m based on amino acid racemization in St. Vincent Gulf (Australia).

Nevertheless, many recent studies have pointed towards the higher end of the range, with some placing MIS 5a GMSL near or above present-day sea level. Weiss et al. (2022) place MIS 5a GMSL above -12 m, based on the connectivity and depth of shallow straits in the Indo Pacific. Dorale et al. (2010) place peak MIS 5a GMSL at $+1$ m based on speleothem records in Mallorca (Spain). Kampolis et al. (2025) place relative sea level at -0.7 m based on speleothem growth in Greece. Relative sea level in the Florida Keys (USA) is found to be -6 to -1 m, although this does not

account for GIA (Hsia et al., 2024). In sum, recent peak MIS 5a GMSL estimates based on direct sea level proxies vary from ~ -30 to $+1$ m, spanning a wide uncertainty range.

While we found that including SIA reconciles the relative mismatch between Nueva Palmira and Chuy Creek, comparison to current constraints on MIS 5a GMSL places our Río de la Plata SLIP-based GMSL estimates (-3.9 to 13.4 m) on the higher end of the likely MIS 5a GMSL range. The lower range of our GMSL estimate is consistent with recent direct proxy evidence and global assessments suggesting MIS 5a GMSL was close to, or only slightly below, present-day sea level.

4.3. Late holocene and historical sea level

The magnitude of subsidence caused by SIA in the Río de la Plata region at Pleistocene timescales raises the question of whether its effects might also impact sea-level estimates for more recent time periods. While our sediment load model was developed specifically to assess the effect of SIA over a full glacial cycle, we show how the response to sediment loading might affect more recent sea-level observations by considering RSL change caused by SIA on shorelines deposited at 7 ka (coinciding with the Holocene highstand in this area) and from 0.1 ka to present-day (Fig. 6). In our sediment loading scenario, deposition begins to occur within the estuary starting in the Holocene (10.5 ka; see the Methods section for details).

Our models show that SIA may have caused up to 1.4 m of subsidence since 7 ka, mostly on sites close to the Río de la Plata estuary (Supplementary Figure 11). While this signal is ~ 5 times lower than the magnitude of GIA sea-level changes in the area (Supplementary Figure 10), it may help explain the discrepancy between sea-level index points and GIA predictions in the Río de la Plata region (Supplementary Figure 12, see the Supplementary Materials for details).

On shorter time scales, magnitudes of SIA effects (Fig. 6) are not negligible compared to spatial variations in RSL and vertical land motion observed by tide gauges and Global Navigation Satellite Systems (Supplementary Figure 13), which have been interpreted in terms of other regional processes (Frederikse et al., 2021). Tide-gauge data from Buenos Aires and Montevideo, among the longest continuous obser-

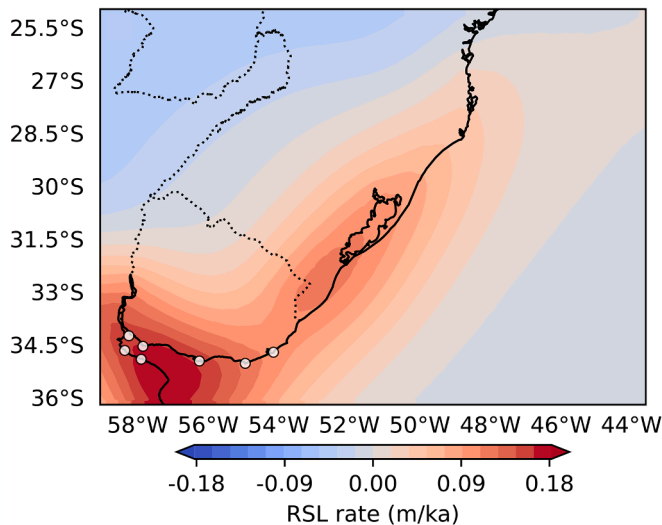


Fig. 6. Rate of Holocene (7 ka - 0 ka) RSL change (positive = land subsidence) caused by SIA (50% loading scenario) in the study area. The dots on the map mark the locations where data from tide gauges records in the Río de la Plata region are available.

variations in the South Atlantic, indicate relative sea-level rise rates of $\sim 1.5 \pm 0.4 \text{ m ka}^{-1}$ and $1.0 \pm 0.3 \text{ m ka}^{-1}$, respectively (Piecuch, 2023). At these tide gauges, streamflow forcing over the twentieth century contributed (0.68 ± 0.47 and $0.41 \pm 0.19 \text{ m ka}^{-1}$ respectively for Buenos Aires and Montevideo, Piecuch, 2023), while GIA-driven sea-level fall over the last 100 years contributes -0.8 ± 0.1 and $-0.7 \pm 0.1 \text{ m ka}^{-1}$, respectively (Dyer et al., 2021). At the same locations, subsidence caused by SIA is between 0.08 and 0.32 m ka^{-1} (25–100% sediment load), reaching in the most extreme loading scenarios magnitudes that are comparable with both GIA and streamflow forcing. On annual to decadal timescales, the contribution of sediment loading to relative sea level will vary depending on the annual Paraná River sediment flux, and more detailed mapping of sedimentation over these timescales will be required to accurately fingerprint the SIA signal in modern tide gauges.

5. Conclusions

In this study, we considered the response of relative sea level to sediment loading (sediment isostatic adjustment; SIA) in the Río de la Plata region. High sediment fluxes from the Paraná River led to the accumulation of $> 100 \text{ m}$ of sediment over the last glacial cycle (122 ka to present day). We show that accounting for sediment isostatic adjustment can resolve the apparent discrepancies between sea level index points across the Río de la Plata estuary dated to MIS 5a ($\sim 80 \text{ ka}$). Furthermore, including corrections for both sediment isostatic assessment and glacial isostatic adjustment improves the fit between MIS5e proxies and global mean sea-level estimates.

The magnitude of sediment isostatic adjustment in the Río de la Plata region is important across multiple timescales. Across the last glacial cycle, sediment loading can explain post-depositional crustal deformation that tilted sea level index points. Over the Holocene, sediment loading contributes over 1 m of RSL, which might help deconvolve the drivers of spatial variability in relative sea level patterns across South America. Modern tide gauges may record relative sea level variations due to sediment loading, and further detailed exploration is necessary to determine the extent to which sedimentation contributes to observed modern sea level gradients between Buenos Aires and Montevideo.

By showing that locally resolved datasets are essential for accurately estimating sediment isostasy, our results highlight the need for expanded shelf coring and seismic surveys to capture the spatial and temporal variability of sediment deposition. Such efforts will enable the

development of improved models of sediment isostasy, capable of reproducing its effects across timescales and refining our understanding of past and future relative sea-level change.

CRedit authorship contribution statement

Alessio Rovere: Writing – review & editing, Writing – original draft, Formal analysis, Conceptualization; **Tamara Pico:** Writing – original draft, Formal analysis, Conceptualization; **Gabriel Tagliaro:** Writing – original draft, Methodology, Formal analysis; **Ciro Cerrone:** Writing – original draft, Formal analysis, Data curation; **Luca Lämmle:** Writing – review & editing, Methodology, Data curation; **Archimedes Perez Filho:** Writing – review & editing, Resources, Methodology; **Karla Rubio-Sandoval:** Writing – review & editing, Investigation, Data curation; **Luigi Jovane:** Writing – review & editing, Resources, Conceptualization; **Jerry X. Mitrovica:** Writing – original draft, Investigation, Conceptualization; **Christopher G. Piecuch:** Writing – review & editing, Investigation, Formal analysis; **Giovanni Scicchitano:** Writing – review & editing, Investigation, Data curation.

Data availability

All data and models used in this work are available from Zenodo at this link: <https://doi.org/10.5281/zenodo.17618912>

Declaration of competing interest

On behalf of the co-authors, I certify that we have NO affiliations with or involvement in any organization or entity with any financial interest (such as honoraria; educational grants; participation in speakers' bureaus; membership, employment, consultancies, stock ownership, or other equity interest; and expert testimony or patent-licensing arrangements), or non-financial interest (such as personal or professional relationships, affiliations, knowledge or beliefs) in the subject matter or materials discussed in this manuscript.

Acknowledgement

This project has received funding from the European Research Council (ERC) under the European Union's Horizon 2020 research and innovation programme (grant agreement no. 802,414 to Alessio Rovere). The manuscript reflects only the view of the authors and the EU is not responsible for any use that may be made of the information it contains. Tamara Pico was supported by the [National Science Foundation](#) (EAR-2120574 and OCE-2054757). Gabriel Tagliaro was supported by Fundação de Amparo à Pesquisa do Estado de São Paulo (FAPESP) grants 2020/08847-6 and 2023/14454-5 and Luigi Jovane acknowledges FAPESP grant 2016/24946-9. Luca Lämmle was supported by FAPESP grant 2023/05346-4. Karla Rubio Sandoval thanks the DGAPA (Dirección General de Asuntos del Personal Académico) for the post-doctoral fellowship, which supported her ongoing research activities. Parts of the data analyses presented in this work were supported by the Marine Science Laboratory of the Department of Earth and Geoenvironmental Sciences at the University of Bari Aldo Moro. Christopher G. Piecuch was supported by the [National Science Foundation](#) (award OCE-2002485) and The GC McConnell Fellowship Fund and The George E. Thibault Early Career Scientist Fund at Woods Hole Oceanographic Institution. Jerry Mitrovica's research was supported by the Lemann Brazil Research Fund at Harvard University. This work was supported by the DoE 2023–2027 (MUR, AIS.DIP.ECCELLENZA2023_27.FF project) through a visiting grant to Ca' Foscari to Luigi Jovane. We thank Jacqueline Austermann (Columbia University) for providing the GIA models used in this work, originally from Dyer et al., 2021. A preprint of this publication was submitted to EarthArxiv. We used ChatGPT (OpenAI) to assist with Python coding (e.g., streamlining scripts, suggesting functions, and drafting markdown cells for Jupyter notebooks) and for improving clarity and readability of the manuscript text. All code and

text generated with AI assistance were thoroughly reviewed, tested, and edited by the authors, who take full responsibility for the final content.

Supplementary material

Supplementary material associated with this article can be found in the online version at [10.1016/j.epsl.2026.119996](https://doi.org/10.1016/j.epsl.2026.119996)

References

- Adams, P.N., Opdyke, N.D., Jaeger, J.M., 2010. Isostatic uplift driven by karstification and sea-level oscillation: modeling landscape evolution in north florida. *Geology* 38 (6), 531–534.
- Alberoni, A., Jeck, I., Silva, C., Torres, L., 2020. The new digital terrain model (DTM) of the brazilian continental margin: detailed morphology and revised undersea feature names. *Geo-Mar. Lett.* 40, 1–16. <https://doi.org/10.1007/s00367-019-00606-x>
- Amsler, M.L., Drago, E.C., 2009. A review of the suspended sediment budget at the confluence of the paran and paraguay rivers. *Hydrol. Process* 23 (22), 3230–3235. <https://doi.org/10.1002/hyp.7390>
- Austermann, J., Mitrovica, J.X., Huybers, P., Rovere, A., 2017. Detection of a dynamic topography signal in last interglacial sea-level records. *Sci. Adv.* 3 (7), e1700457. <https://doi.org/10.1126/sciadv.1700457>
- Bahr, D.B., Hutton, E. W.H., Syvitski, J. P.M., Pratson, L.F., 2001. Exponential approximations to compacted sediment porosity profiles. *Comput. Geosci.* 27 (6), 691–700.
- Barnett, R.L., Austermann, J., Dyer, B., Telfer, M.W., Barlow, N. L.M., Boulton, S.J., Carr, A.S., Creel, R.C., 2023. Constraining the contribution of the antarctic ice sheet to last interglacial sea level. *Sci. Adv.* 9 (27), ead0198. Publisher: American Association for the Advancement of Science.
- Braun, J., 2010. The many surface expressions of mantle dynamics. *Nat. Geosci.* 3 (12), 825–833. Publisher: Springer Science and Business Media LLC. <https://doi.org/10.1038/ngeo1020>
- Brunetto, E., Sobrero, F.S., Gimenez, M.E., 2019. Quaternary deformation and stress field in the Ro de la Plata craton (southeastern south america). *J. South Am. Earth Sci.* 91, 332–351. <https://doi.org/10.1016/j.jsames.2017.04.010>
- Colleoni, F., Wekerle, C., Naslund, J.-O., Brandefelt, J., Masina, S., 2016. Constraint on the penultimate glacial maximum northern hemisphere ice topography (≈ 140 kyrs BP). *Quat. Sci. Rev.* 137, 97–112.
- Creveling, J.R., Austermann, J., Dutton, A., 2019. Uplift of trail ridge, florida, by karst dissolution, glacial isostatic adjustment, and dynamic topography. *J. Geophys. Res. Solid Earth* 124 (12), 13354–13366.
- Creveling, J.R., Mitrovica, J.X., Clark, P.U., Waelbroeck, C., Pico, T., 2017. Predicted bounds on peak global mean sea level during marine isotope stages 5a and 5c. *Quat. Sci. Rev.* 163, 193–208. <https://doi.org/10.1016/j.quascirev.2017.03.003>
- Dalca, A.V., Ferrier, K.L., Mitrovica, J.X., Perron, J.T., Milne, G.A., Creveling, J.R., 2013. On postglacial sea level-III incorporating sediment redistribution. *Geophys J. Int.* 194 (1), 45–60. <https://doi.org/10.1093/gji/ggt089>
- Dalton, A.S., Pico, T., Gowan, E.J., Clague, J.J., Forman, S.L., McMartin, I., Sarala, P., Helmens, K.F., 2022. The marine $\delta^{18}O$ record overestimates continental ice volume during marine isotope stage 3. *Glob. Planet Change* 212, 103814.
- De Gelder, G., Husson, L., Pastier, A.-M., Fernandez-Blanco, D., Pico, T., Chauveau, D., Authemayou, C., Pedoja, K., 2022. High interstadial sea levels over the past 420ka from the huon peninsula, papua new guinea. *Commun. Earth & Environ.* 3 (1), 256. <https://doi.org/10.1038/s43247-022-00583-7>
- Depetris, P.J., Griffin, J.J., 1968. Suspended load in the ro de la plata drainage basin. *Sedimentology* 11 (1–2), 53–60. <https://doi.org/10.1111/j.1365-3091.1968.tb00840.x>
- Dorale, J.A., Onac, B.P., Fornos, J.J., Gines, J., Gines, A., Tuccimei, P., Peate, D.W., 2010. Sea-level highstand 81,000 years ago in mallorca. *Science* 327 (5967), 860–863.
- Dutton, A., Carlson, A.E., Long, A.J., Milne, G.A., Clark, P.U., DeConto, R., Horton, B.P., Rahmstorf, S., Raymo, M.E., 2015. Sea-level rise due to polar ice-sheet mass loss during past warm periods. *Science* 349 (6244), aaa4019. Publisher: American Association for the Advancement of Science.
- Dyer, B., Austermann, J., D’Andrea, W.J., Creel, R.C., Sandstrom, M.R., Cashman, M., Rovere, A., Raymo, M.E., 2021. Sea-level trends across the bahamas constrain peak last interglacial ice melt. *Proc. Natl. Acad. Sci. U.S.A.* 118 (33), 1–11. <https://doi.org/10.1073/pnas.2026839118>
- Dziewonski, A.M., Anderson, D.L., 1981. Preliminary reference earth model. *Phys. Earth Planet. Inter.* 25 (4), 297–356.
- Farmer, J.R., Pico, T., Underwood, O.M., Cleveland Stout, R., Granger, J., Cronin, T.M., Fripiat, F., Martinez-Garca, A., Haug, G.H., Sigman, D.M., 2023. The bering strait was flooded 10,000 years before the last glacial maximum. *Proc. Natl. Acad. Sci.* 120 (1), e2206742119.
- Farrell, W.E., Clark, J.A., 1976. On postglacial sea level. *Geophys J. Int.* 46 (3), 647–667.
- Ferrier, K.L., Austermann, J., Mitrovica, J.X., Pico, T., 2017. Incorporating sediment compaction into a gravitationally self-consistent model for ice age sea-level change. *Geophys J. Int.* 211 (1), 663–672. <https://doi.org/10.1093/gji/ggx293>
- Ferrier, K.L., Mitrovica, J.X., Giosan, L., Clift, P.D., 2015. Sea-level responses to erosion and deposition of sediment in the indus river basin and the arabian sea. *Earth Planet. Sci. Lett.* 416, 12–20. <https://doi.org/10.1016/j.epsl.2015.01.026>
- Fossati, M., Cayocca, F., Piedra-Cueva, I., 2014. Fine sediment dynamics in the Ro de la Plata. *Adv. Geosci.* 39, 75–80. <https://doi.org/10.5194/adgeo-39-75-2014>
- Frederikse, T., Adhikari, S., Daley, T.J., Dangendorf, S., Gehrels, R., Landerer, F., Marcos, M., Newton, T.L., Rush, G., Slangen, A. B.A., Woppelmann, G., 2021. Constraining 20th-century sea-level rise in the south atlantic ocean. *J. Geophys. Res. Oceans* 126 (3), e2020JC016970. e2020JC016970 2020JC016970. <https://doi.org/10.1029/2020JC016970>
- Grant, K.M., Rohling, E.J., Ramsey, C.B., Cheng, H., Edwards, R.L., Florindo, F., Heslop, D., Marra, F., Roberts, A.P., Tamisiea, M.E., Williams, F., 2014. Sea-level variability over five glacial cycles. *Nat. Commun.* 5 (1), 5076. <https://doi.org/10.1038/ncomms6076>
- Gregory, J.M., Griffies, S.M., Hughes, C.W., Lowe, J.A., Church, J.A., Fukimori, I., Gomez, N., Kopp, R.E., Landerer, F., Cozannet, G.L., Ponte, R.M., Stammer, D., Tamisiea, M.E., van de Wal, R. S.W., 2019. Concepts and terminology for sea level: mean, variability and change, both local and global. *Surv. Geophys.* 40 (6), 1251–1289. <https://doi.org/10.1007/s10712-019-09525-z>
- Guedes, C. C.F., Nascimento, M. G.D., Angulo, R.J., Souza, M. C.D., 2020. Geological evidences as a guide to OSL dating interpretation and northern occurrence of MIS 7e barrier at southern brazil. *J. South Am. Earth Sci.* 98, 102478. <https://doi.org/10.1016/j.jsames.2019.102478>
- Gulev, S.K., Thorne, P.W., Ahn, J., Dentener, F.J., Domingues, C.M., Gerland, S., Gong, D., Kaufman, D.S., Nnamchi, H.C., Quaas, J., Rivera, J.A., Sathyendranath, S., Smith, S.L., Trewin, B., von Schuckmann, K., Vose, R.S., 2021. Changing State of the Climate System. Cambridge University Press, Cambridge, United Kingdom and New York, NY, USA. p. 287–422. <https://doi.org/10.1017/9781009157896.004>
- Hsia, S., Toth, L.T., Mortlock, R., Kerans, C., 2024. Re-evaluating marine isotope stage 5a paleo-sea-level trends from across the florida keys reef tract. *Quat. Sci. Adv.* 15, 100222. <https://doi.org/10.1016/j.qsa.2024.100222>
- Kampolis, I., Triantafyllidis, S., Polyak, V.J., Asmerom, Y., Onac, B.P., 2025. Sea level during marine isotope stage 5a in the messiniakos gulf (peloponnese peninsula, greece). *Geomorphology* 486, 109911.
- Laborde, J.L., Nagy, G.J., 1999. Hydrography and sediment transport characteristics of the Ro de la Plata: a review. In: Perillo, G. M.E., Piccolo, M.C., Pino-Quirova, M. (Eds.), *Estuaries of South America*. Springer Berlin Heidelberg, Berlin, Heidelberg, pp. 133–159. https://doi.org/10.1007/978-3-642-60131-6_7
- Lambeck, K., Chappell, J., 2001. Sea level change through the last glacial cycle. *Science* 292 (5517), 679–686. <https://doi.org/10.1126/science.1059549>
- Lambeck, K., Purcell, A., Funder, S., Kjær, K.H., Larsen, E., Moller, P., 2006. Constraints on the late saalian to early middle weichselian ice sheet of eurasia from field data and rebound modelling. *Boreas* 35 (3), 539–575.
- Lantzsch, H., Hanebuth, T. J.J., Chiessi, C.M., Schwenk, T., Violante, R.A., 2014. The high-supply, current-dominated continental margin of southeastern south america during the late quaternary. *Quat. Res.* 81 (2), 339–354. <https://doi.org/10.1016/j.yqres.2014.01.003>
- Lin, Y., Whitehouse, P.L., Hibbert, F.D., Woodroffe, S.A., Hinestrosa, G., Webster, J.M., 2023. Relative sea level response to mixed carbonate-siliciclastic sediment loading along the great barrier reef margin. *Earth Planet. Sci. Lett.* 607, 118066.
- Lopes, R.P., Dillenburg, S.R., Schultz, C.L., Ferigolo, J., Ribeiro, A.M., Pereira, J.C., Holanda, E.C., Pitana, V.G., Kerber, L., 2014. The sea-level highstand correlated to marine isotope stage (MIS) 7 in the coastal plain of the state of Rio grande do sul, brazil. *Anais da Academia Brasileira de Ciencias* 86 (4), 1573–1595. <https://doi.org/10.1590/0001-3765201420130274>
- Lopes, R.P., Pereira, J.C., Caron, F., Dillenburg, S.R., Rosa, M. L. C. D.C., Barboza, E.G., Savian, J.F., Sawakuchi, A.O., Tatum, S.H., Yee, M., 2024. Stratigraphy and evolution of the late pleistocene (MIS 5) coastal barrier III in southern brazil. *Quat. Res.* <https://doi.org/10.1017/qua.2023.67>
- Lopes, R.P., Pereira, J.C., Kinoshita, A., Mollembreg, M., Barbosa, F., Baffa, O., 2020. Geological and taphonomic significance of electron spin resonance (ESR) ages of middle-late pleistocene marine shells from barrier-lagoon systems of southern brazil. *J. South Am. Earth Sci.* 101, 102605. <https://doi.org/10.1016/j.jsames.2020.102605>
- Martnez, S., Ubilla, M., Verde, M., Perea, D., Rojas, A., Guerquiz, R., Pieiro, G., 2001. Paleocology and geochronology of uruguayan coastal marine pleistocene deposits. *Quat. Res.* 55 (2), 246–254. <https://doi.org/10.1006/qres.2000.2204>
- Michaelovitch De Mahiques, M., Violante, R., Franco-Fraguas, P., Burone, L., Barbedo Rocha, C., Ortega, L., Felicio Dos Santos, R., Mi Kim, B.S., Lopes Figueira, R.C., Caruso Bicego, M., 2021. Control of oceanic circulation on sediment distribution in the southwestern atlantic margin (23 to 55 s). *Ocean Sci.* 17 (5), 1213–1229. <https://doi.org/10.5194/os-17-1213-2021>
- Milne, G.A., Mitrovica, J.X., 1998. Postglacial sea-level change on a rotating earth. *Geophys J. Int.* 133 (1), 1–19. Publisher: Oxford University Press (OUP). <https://doi.org/10.1046/j.1365-246x.1998.1331455.x>
- Mix, A.C., 1987. Hundred-kiloyear cycle queried. *Nature* 327 (6121), 370–370.
- Muhs, D.R., Simmons, K.R., Schumann, R.R., Groves, L.T., Mitrovica, J.X., Laurel, D., 2012. Sea-level history during the last interglacial complex on san nicolas island, california: implications for glacial isostatic adjustment processes, paleoecogeography and tectonics. *Quat. Sci. Rev.* 37, 1–25. <https://doi.org/10.1016/j.quascirev.2012.01.010>
- Murray-Wallace, C.V., Cann, J.H., Yokoyama, Y., Nicholas, W.A., Lachlan, T.J., Pan, T.-Y., Dosseto, A., Belperio, A.P., Gostin, V.A., 2021. Late pleistocene interstadial sea-levels (MIS 5a) in gulf st vincent, southern australia, constrained by amino acid racemization dating of the benthic foraminifer elphidium macelliforme. *Quat. Sci. Rev.* 259, 106899.
- Peak, B.A., Latychev, K., Hoggard, M.J., Mitrovica, J.X., 2022. Glacial isostatic adjustment in the red sea: impact of 3-d earth structure. *Quat. Sci. Rev.* 280, 107415. <https://doi.org/10.1016/j.quascirev.2022.107415>
- Pedoja, K., Husson, L., Regard, V., Cobbold, P.R., Ostanciaux, E., Johnson, M.E., Kershaw, S., Saillard, M., Martinod, J., Furgerot, L., Weill, P., Delcaillau, B., 2011a. Relative sea-level fall since the last interglacial stage: are coasts uplifting worldwide? *Earth Sci. Rev.* 108 (1), 1–15. <https://doi.org/10.1016/j.earscirev.2011.05.002>
- Pedoja, K., Regard, V., Husson, L., Martinod, J., Guillaume, B., Fucks, E., Iglesias, M., Weill, P., 2011b. Uplift of quaternary shorelines in eastern patagonia: darwin revisited. *Geomorphology* 127 (3), 121–142. <https://doi.org/10.1016/j.geomorph.2010.08.003>

- Peltier, W.R., Argus, D.F., Drummond, R., 2015. Space geodesy constrains ice age terminal deglaciation: the global ICE-6g_c (VM5a) model. *J. Geophys. Res. Solid Earth* 120 (1), 450–487.
- Pereira De Ávila, A.S., Leonhardt, A., Diniz, D., 2020. Paleoenvironmental reconstruction off southern Brazil during a glacial period (66.5–47 kyr BP): continental and oceanic environments. *J. Coastal Res.* 36 (6). <https://doi.org/10.2112/JCOASTRES-D-19-00074.1>
- Perez, L., García-Rodríguez, F., Hanebuth, T. J.J., 2016. Variability in terrigenous sediment supply offshore of the río de la plata (Uruguay) recording the continental climatic history over the past 1200 years. *Clim. Past* 12 (3), 623–634. <https://doi.org/10.5194/cp-12-623-2016>
- Pico, T., 2020. Towards assessing the influence of sediment loading on last interglacial sea level. *Geophys. J. Int.* 220 (1), 384–392.
- Pico, T., 2022. Toward new and independent constraints on global mean sea-level highstands during the last glaciation (marine isotope stage 3, 5a, and 5c). *Paleoceanography Paleoclimatology*. 37 (12), e2022PA004560.
- Pico, T., Mitrovica, J.X., Ferrier, K.L., Braun, J., 2016. Global ice volume during MIS 3 inferred from a sea-level analysis of sedimentary core records in the yellow river delta. *Quat. Sci. Rev.* 152, 72–79. <https://doi.org/10.1016/j.quascirev.2016.09.012>
- Piecuch, C.G., 2023. River effects on sea-level rise in the río de la plata estuary during the past century. *Ocean Sci.* 19 (1), 57–75. <https://doi.org/10.5194/os-19-57-2023>
- Poirier, R.K., Gaetano, M.Q., Acevedo, K., Schaller, M.F., Raymo, M.E., Kozdon, R., 2021. Quantifying diagenesis, contributing factors, and resulting isotopic bias in benthic foraminifera using the foraminiferal preservation index: implications for geochemical proxy records. *Paleoceanography and Paleoclimatology* 36 (5), e2020PA004110.
- Reynolds, D.J., Steckler, M.S., Coakley, B.J., 1991. The role of the sediment load in sequence stratigraphy: the influence of flexural isostasy and compaction. *J. Geophys. Res. Solid Earth* 96 (B4), 6931–6949. <https://doi.org/10.1029/90JB01914>
- Rojas, A., Martínez, S., 2016. Marine isotope stage 3 (MIS 3) versus marine isotope stage 5 (MIS 5) fossiliferous marine deposits from Uruguay. In: Gasparini, G.M., Rabassa, J., Deschamps, C., Tonni, E.P. (Eds.), *Marine Isotope Stage 3 in Southern South America*, 60 KA B.P.–30 KA B.P.. Springer International Publishing, Cham, pp. 249–278. Series Title: Springer Earth System Sciences. https://doi.org/10.1007/978-3-319-40000-6_14
- Rovere, A., Pico, T., Richards, F., O’Leary, M.J., Mitrovica, J.X., Goodwin, I.D., Austermann, J., Latychev, K., 2023. Influence of reef isostasy, dynamic topography, and glacial isostatic adjustment on sea-level records in northeastern Australia. *Commun. Earth Environ.* 4 (1), 328.
- Rovere, A., Stocchi, P., Vacchi, M., 2016. Eustatic and relative sea level changes. *Curr. Clim. Change Rep* 2 (4), 221–231.
- Ryan, W. B.F., Carbotte, S.M., Coplan, J.O., O’Hara, S., Melkonian, A., Arko, R., Weisell, R.A., Ferrini, V., Goodwillie, A., Nitsche, F., et al., 2009. Global multi-resolution topography synthesis. *Geochem. Geophys. Geosyst.* 10 (3).
- Shackleton, S., Menking, J.A., Brook, E., Buizert, C., Dyonisius, M.N., Petrenko, V.V., Baggenstos, D., Severinghaus, J.P., 2021. Evolution of mean ocean temperature in marine isotope stage 4. *Clim. Past* 17 (5), 2273–2289.
- Shackleton, S., Seltzer, A., Baggenstos, D., Lisiecki, L.E., 2023. Benthic $\delta^{18}O$ records earth’s energy imbalance. *Nat. Geosci.* 16 (9), 797–802.
- Shakun, J.D., Clark, P.U., He, F., Lifton, N.A., Liu, Z., Otto-Bliesner, B.L., 2015. Regional and global forcing of glacier retreat during the last deglaciation. *Nat. Commun.* 6 (1), 8059.
- Simms, A.R., Anderson, J.B., DeWitt, R., Lambeck, K., Purcell, A., 2013. Quantifying rates of coastal subsidence since the last interglacial and the role of sediment loading. *Glob. Planet. Change* 111, 296–308. <https://doi.org/10.1016/j.gloplacha.2013.10.002>
- Simms, A.R., Rouby, H., Lambeck, K., 2016. Marine terraces and rates of vertical tectonic motion: the importance of glacio-isostatic adjustment along the Pacific coast of central North America. *Bulletin* 128 (1–2), 81–93. Publisher: Geological Society of America.
- Spratt, R.M., Lisiecki, L.E., 2016. A late Pleistocene sea level stack. *Clim. Past* 12 (4), 1079–1092. <https://doi.org/10.5194/cp-12-1079-2016>
- Stephenson, S.N., White, N.J., Li, T., Robinson, L.F., 2019. Disentangling interglacial sea level and global dynamic topography: analysis of Madagascar. *Earth Planet. Sci. Lett.* 519, 61–69.
- Tagliaro, G., Britzke, A., Gama, M. A.C., Bauli, P., Negrão, A.P., Jovane, L., 2024. Neogene evolution of the margin adjacent to the La Plata river delta (Pelotas basin): sedimentary pathways and the origins of the Rio Grande cone. *Basin Res.* 36 (1), e12848. <https://doi.org/10.1111/bre.12848>
- Tawil-Morsink, K., Austermann, J., Dyer, B., Dumitru, O.A., Precht, W.F., Cashman, M., Goldstein, S.L., Raymo, M.E., 2022. Probabilistic investigation of global mean sea level during MIS 5a based on observations from Cave Hill, Barbados. *Quat. Sci. Rev.* 295, 107783. <https://doi.org/10.1016/j.quascirev.2022.107783>
- Thompson, S.B., Creveling, J.R., 2021. A global database of marine isotope substage 5a and 5c marine terraces and paleoshoreline indicators. *Earth Syst. Sci. Data* 13 (7), 3467–3490. <https://doi.org/10.5194/essd-13-3467-2021>
- Thompson, S.B., Creveling, J.R., Latychev, K., Mitrovica, J.X., 2023. Three-dimensional glacial isostatic adjustment modeling reconciles conflicting geographic trends in North American marine isotope stage 5a relative sea level observations. *Geology* 51 (9), 808–812. <https://doi.org/10.1130/G51257.1>
- Tomazelli, L.J., Dillenburg, S.R., 2007. Sedimentary facies and stratigraphy of a last interglacial coastal barrier in South Brazil. *Mar. Geol.* 244 (1–4), 33–45.
- Tomazelli, L.J., Dillenburg, S.R., Villwock, J.A., 2006. Geological evolution of Rio Grande do Sul coastal plain, southern Brazil. *J. Coastal Res.* , 275–278.
- Törnqvist, T.E., Wallace, D.J., Storms, J. E.A., Wallinga, J., Van Dam, R.L., Blauw, M., Derksen, M.S., Klerks, C. J.W., Meijneken, C., Snijders, E. M.A., 2008. Mississippi delta subsidence primarily caused by compaction of Holocene strata. *Nat. Geosci.* 1 (3), 173–176.
- Villwock, J.A., 1984. Geology of the coastal province of Rio Grande do Sul, southern Brazil. a synthesis. *Pesquisas em Geociências* 16 (16), 5–49.
- Waelbroeck, C., Labeyrie, L., Michel, E., Duplessy, J.-C., McManus, J.F., Lambeck, K., Balbon, E., Labracherie, M., 2002. Sea-level and deep water temperature changes derived from benthic foraminifera isotopic records. *Quat. Sci. Rev.* 21 (1–3), 295–305.
- Weiss, T.L., Linsley, B.K., Gordon, A.L., Rosenthal, Y., Dannenmann-Di Palma, S., 2022. Constraints on marine isotope stage 3 and 5 sea level from the flooding history of the Karimata Strait in Indonesia. *Paleoceanogr. Paleoclimatol.* 37 (9), e2021PA004361.